1592
doi:10.1017/S1431927620018644
Microsc. Microanal. 26 (Suppl 2), 2020

Challenges and Solutions in the Characterization of Hierarchically Structured, Functionally Graded Tooth Biominerals

Karen DeRocher[1], Paul Smeets[1], Berit Goodge[2], Michael Zachman[3], Prasanna Balachandran[4], Linus Stegbauer[1], Michael Cohen[1], Lyle Gordon[1], James Rondinelli[1], Lena Kourkoutis[2] and Derk Joester[1]

[1]Northwestern University, Evanston, Illinois, United States, [2]Cornell University, Ithaca, New York, United States, [3]Oak Ridge National Laboratory, Oak Ridge, Tennessee, United States, [4]University of Virginia, Charlottesville, Virginia, United States

Dental enamel is a principal component of our teeth, providing protection to the underlying dentin. It has evolved to bear large masticatory forces, resist mechanical fatigue, and withstand wear over decades of use. However, as an acellular tissue, it lacks some of the sophisticated self-repair capabilities of other mineralized tissues such as bone. Functional impairment or loss of enamel, for instance as a consequence of developmental defects or tooth decay (caries), has a dramatic impact on health and quality of life, and causes significant costs to society.[1] The ability to characterize the chemically complex microstructure of enamel is fundamentally enabling research targeted at improving caries prophylaxis and early/non-invasive intervention, understanding developmental mechanisms, and developing novel and/or bio-inspired materials.

Enamel covers the entire crown of human teeth (**Figure 1**), and can reach a thickness of several millimeters. A characteristic microstructural element is the enamel rod, which in turn is comprised of thousands of lath-like crystallites that are aligned with their crystallographic *c*-direction approximately parallel to the long axis of the rod. Crystallites sectioned normal to their long axis appear as oblong, convex polygons with an edge length of 20-50 nm in the short and 70-170 nm in the long direction. The extraordinary mechanical performance of enamel, including its surprising fracture toughness, is thought to emerge from a combination of factors at different levels of hierarchy.[2]

Nominally comprised of hydroxylapatite (OHAp; $Ca_5(PO_4)_3(OH)$), minor enamel constituents include magnesium (0.2 – 0.6 wt%), sodium (0.2 – 0.9 wt%), carbonate (2.7 – 5 wt%), and fluoride (~0.01 wt%).[3] Recently, it was discovered in rodent incisor enamel that most Mg is not incorporated into crystallites, but confined between them as Mg-substituted amorphous calcium phosphate (Mg-ACP).[4,5] The high solubility of Mg-ACP is responsible for the highly anisotropic etching behavior of rodent enamel. Segregation of Mg to grain boundaries in human enamel was confirmed by APT [6], however, the existence of Mg-ACP has not yet been demonstrated. Little is known about the distribution of the other minor constituents, but circumstantial evidence points to inhomogeneities in their distribution even at the level of individual crystallites.

Quantitative chemical imaging of enamel at thus length scale is a formidable challenge. This is because the elements of interest have relatively low atomic number, are present at low abundance (< 1 at%), and occur in a matrix that is highly prone to beam-induced damage. I will discuss specific challenges we encountered when using STEM-ADF, -EDS, and -EELS techniques for high-resolution structural and chemical imaging and how we managed to overcome some of them using cryogenic imaging.[7] I will further discuss how STEM techniques in conjunction with UV-laser pulsed atom probe tomography (APT) has given us remarkable new insights into nanoscale structure and composition of human enamel. Specifically, I will confirm the existence of an amorphous intergranular phase that cements

together crystallites in human enamel. I will further describe highly characteristic gradients of Mg^{2+}, Na^{+}, CO_3^{2-}, and F^{-} across individual crystallites that result in a sandwich core-shell structure (**Figure 2**). Finally, I will discuss implications of this structure for the mechanical properties of enamel, and report on our exploration of residual stresses (using DFT and FEM modeling) in enamel, its dissolution behavior, and implications for enamel formation during tooth development.[8]

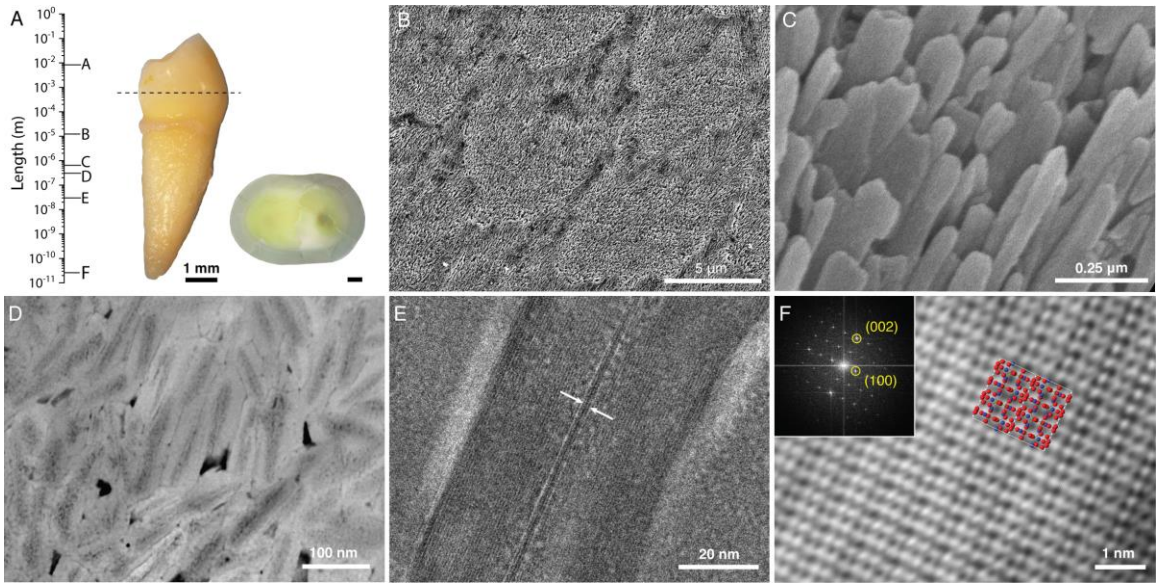

Figure 1. Microstructure of human enamel. A. Human premolar and section parallel to the mid-coronal cervical plane. B. SEM image showing enamel rods and inter-rod enamel in lactic acid-etched outer enamel. C. SEM image of enamel crystallites. D-E. STEM-ADF image of enamel crystallites in cross section. F. Cryo-STEM-ADF lattice image of a crystallite oriented parallel to the [010] zone axis with 2×2×2 OHAp supercell (Ca, blue; O, red; P, green; H, white).

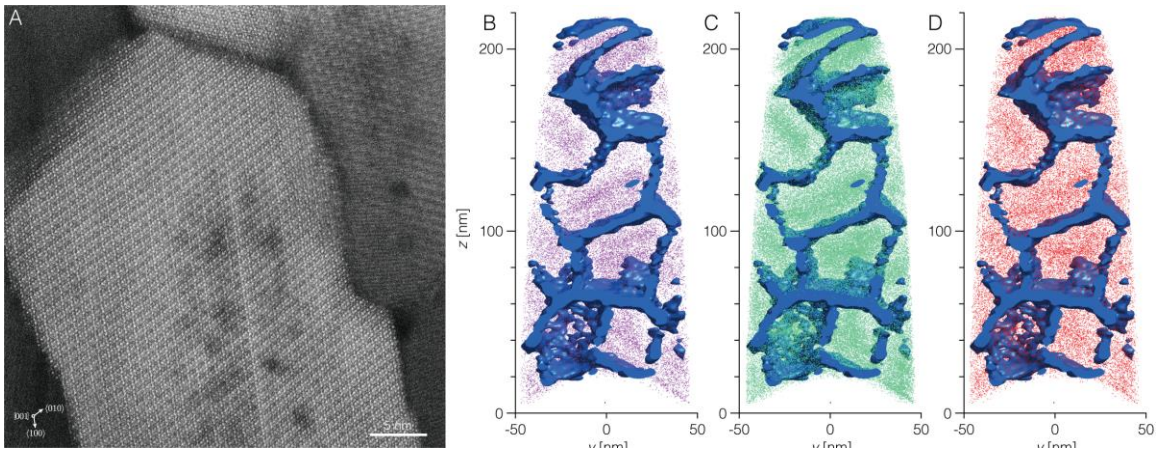

Figure 2. Atomic Scale Imaging of Enamel Crystallites. A. Aberration-corrected cryo-STEM MAADF lattice image (unfiltered; single frame) with partial view of several crystallites. The crystallite that appears bright is oriented along the [001] zone axis. B-D. 3D reconstructions of atom probe tomography data sets showing several crystallites in cross section. Distribution of CaF+ ions is indicated by an iso-concentration surface (0.1 nm-3, blue). Positions of individual 24Mg2+ (A), 23Na+(B), and carbonate-derived ions (COxHy+, C) are indicated.

https://doi.org/10.1017/S1431927620018644 Published online by Cambridge University Press

References

[1] O. D. Klein, O. Duverger, W. Shaw, R. S. Lacruz, D. Joester, J. Moradian-Oldak, M. K. Pugach, J. T. Wright, S. E. Millar, A. B. Kulkarni, J. D. Bartlett, T. G. H. Diekwisch, P. DenBesten, J. P. Simmer, *Int J Oral Sci* **2017**, *9*, e3.
[2] E. D. Yilmaz, G. A. Schneider, M. V. Swain, *Phil. Trans. Royal Soc. A* **2015**, *373*.
[3] C. Robinson, R. C. Shore, S. J. Brookes, S. Strafford, S. R. Wood, J. Kirkham, Crit Rev Oral Biol Med 2000, 11, 15. "*The Chemistry of Enamel Caries*".
[4] Gordon, Cohen, MacRenaris, Pasteris, Seda, Joester, *Science* **2015**, *347*, 746-750.
[5] Gordon, Joester, *Front Physiol* **2015**, *6*.
[6] A. La Fontaine, A. Zavgorodniy, H. Liu, R. Zheng, M. Swain, J. Cairney, *Sci. Adv.* **2016**, *2*.
[7] Smeets, DeRocher, Zachman, Goodge, Kourkoutis, Joester, *Microsc Microanal* **2018**, *24*, 1266-1267.
[8] This work was supported by NIH-NIDCR (R01 DE025702-01, R03 DE025303-01); NSF (DMR-1508399, DMR-1539918); DFG (STE2689/1-1) and used facilities supported by ONR (N00014-1712870) and NSF (DMR-1720139, ECCS-1542205, DMR-1719875, MRI-1429155), among others.